THE JOURNAL OF BIOLOGICAL CHEMISTRY
Vol. 271, No. 25, Issue of June 21, pp. 15091–15098, 1996

Printed in U.S.A.

cDNA Cloning of the Hepatocyte Canalicular Isoform of the Multidrug Resistance Protein, cMrp, Reveals a Novel Conjugate Export Pump Deficient in Hyperbilirubinemic Mutant Rats*

(Received for publication, March 7, 1996)

Markus Büchler‡, Jörg König‡, Manuela Brom‡, Jürgen Kartenbeck‡, Herbert Spring‡, Toru Horie§, and Dietrich Keppler‡¶

From the ‡Deutsches Krebsforschungszentrum, D-69120 Heidelberg, Federal Republic of Germany and the §Eisai Research Laboratories, Ibaraki 300-21, Japan

ATP-dependent transport of glutathione and glucuronate conjugates from hepatocytes into bile is mediated by a distinct member of the ATP-binding cassette superfamily. We have cloned and sequenced the canalicular isoform of the multidrug resistance protein from rat liver, and termed it cMrp. This membrane glycoprotein is composed of 1541 amino acids with an identity of 47.8% with the human multidrug resistance protein (MRP) and of 41.9% with the yeast cadmium factor (YCF1). The carboxyl-terminal 130 amino acids of the human hepatocyte canalicular isoform of MRP (cMRP) were 80.2% identical with rat cMrp.

cMrp was not expressed in the liver of two mutant rat strains, the Eisai hyperbilirubinemic rat and the GY/TR$^-$ mutant, which are deficient in the ATP-dependent transport of conjugates across the canalicular membrane. Immunoblotting using an antibody raised against the carboxyl terminus of cMrp detected the glycoprotein of about 190 kDa only in the canalicular membrane from normal liver. Double immunofluorescence and confocal laser scanning microscopy localized cMrp exclusively to the canalicular membrane domain of hepatocytes and demonstrated its loss in the hyperbilirubinemic mutant rat. The results identify cMrp as a canalicular transport protein with a novel sequence and with a function similar to the one of the MRP.

The multidrug resistance protein (MRP)[1] was originally cloned and sequenced from multidrug-resistant human lung cancer cells and identified as an integral membrane glycoprotein of about 190 kDa belonging to the superfamily of ATP-binding cassette transporters (1). Primary active ATP-dependent transport of amphiphilic anions, particularly of conjugates of lipophilic substances with glutathione, glucuronate, or sulfate, has been recognized as the function of MRP as studied in plasma membrane vesicles (2–6). An isoform of MRP has been identified in the hepatocyte canalicular membrane by immunoblotting, immunofluorescence microscopy, and sequencing of cDNA fragments (7). The hepatocyte canalicular membrane is a site of active transport of substances from the liver into bile. The canalicular isoform of Mrp was not detected in the mutant rat strain GY/TR$^-$ (7) which is deficient in the secretion of anionic conjugates from the liver into bile (8). Reverse transcription PCR indicated the apparent loss of one Mrp-related mRNA species in the liver of the GY/TR$^-$ mutant rats (7). These studies provided the basis for the cloning and sequencing of the full-length cDNA encoding the rat hepatocyte canalicular isoform of Mrp (cMrp) reported in the present study. We describe, in addition, the absence of cMrp in another strain of mutant rats, the Eisai hyperbilirubinemic rat (EHBR). Similar as the GY/TR$^-$ mutant rats (8), the EHBR mutants are characterized by an impaired secretion of anionic conjugates, including bilirubin glucuronide, from the hepatocytes into bile (9, 10) and by the lack of ATP-dependent conjugate transport by canalicular plasma membrane vesicles (11).

The sequence of rat cMrp reported below represents a novel ATP-binding cassette transporter, which we compare to the related MRP sequence determined by Cole *et al.* (1) as well as to the yeast cadmium resistance transport protein YCF1 (12). Moreover, we deduced the carboxyl-terminal sequence of the human hepatocyte canalicular MRP isoform, cMRP, from a cDNA clone isolated from human liver. This has been of particular interest since the hereditary deficiency of the hepatocyte canalicular conjugate export pump in humans is considered to be the basis of the Dubin-Johnson syndrome (13) which is characterized by a selective abnormality in the excretion of conjugated anions into the bile and by a chronic conjugated hyperbilirubinemia (14).

EXPERIMENTAL PROCEDURES

Materials—[14,15,19,20-$^3H_4$]LTC_4 (4.7 Tbq/mmol), [α-^{32}P]dCTP (111 Tbq/mmol), and α-^{35}S-dATP (37 Tbq/mmol) were obtained from DuPont NEN. The Rediprime DNA labeling system was from Amersham-Buchler (Braunschweig, Germany). The LTD_4 receptor antagonist and transport inhibitor MK 571 was kindly provided by Dr. A. W. Ford-

* This work was supported in part by the Deutsche Forschungsgemeinschaft through SFB 352/B3, by the Forschungsschwerpunkt Transplantation, Heidelberg, and by the Fonds der Chemischen Industrie, Frankfurt, Germany. The costs of publication of this article were defrayed in part by the payment of page charges. This article must therefore be hereby marked "*advertisement*" in accordance with 18 U.S.C. Section 1734 solely to indicate this fact.

The nucleotide sequence(s) reported in this paper has been submitted to the GenBank™/EBI Data Bank with accession number(s) X90643 (seq1), X90642 (seq2), X96393 (cMrp), and X96395 (3′-end of cMRP).

¶ To whom correspondence should be addressed: Division of Tumor Biochemistry, Deutsches Krebsforschungszentrum, Im Neuenheimer Feld 280, D-69120 Heidelberg, Germany. Tel.: 49/6221-422400; Fax: 49/6221-422402; E-mail: d.keppler@dkfz-heidelberg.de.

[1] The abbreviations used are: MRP, human multidrug resistance protein; *MRP*, gene encoding the human multidrug resistance protein; *mrp*, gene encoding the rat multidrug resistance protein; Mrp, rat multidrug resistance protein; ABC, ATP-binding cassette; cMRP, human canalicular isoform of the multidrug resistance protein; cMrp, rat canalicular isoform of the multidrug resistance protein; *cmrp*, gene encoding the rat canalicular multidrug resistance protein; DPPIV, dipeptidyl peptidase IV (CD26; EC 3.4.14.5); EHBR, Eisai hyperbilirubinemic rat (9, 10); GY, Groningen Yellow; GY/TR$^-$, transport-deficient Wistar rat (8); LT, leukotriene; MK 571, 3-([{3-(2-[7-chloro-2-quinolinyl]ethenyl)phenyl}-{(3-dimethyl-amino-3-oxopropyl)-thio}-methyl]thio) propanoic acid; RACE, rapid amplification of cDNA ends; RT, reverse transcription; PCR, polymerase chain reaction; TM, transmembrane; bp, base pair(s); kb, kilobase pair(s).

Hutchinson (Merck-Frosst Centre for Therapeutic Research, Pointe Claire-Dorval, Quebec, Canada). The protein standard mixture (M_r 43,000–200,000) for SDS-polyacrylamide gel electrophoresis was from Merck (Darmstadt, Germany). Nitrocellulose filters (pore size 0.2 μm) were from Schleicher & Schuell (Dassel, Germany).

Antibodies—The EAG15 polyclonal antibody was raised against the 12-amino acid peptide sequence (EAGIENVNHTEL) at the carboxyl terminus of the rat cMrp sequence. The peptide was synthesized automatically (ABI 430A peptide synthesizer, Applied Biosystems) under previously published conditions (15) with an additional cysteine residue at the amino-terminal end of the peptide. After coupling to maleimide-activated keyhole limpet hemocyanin (Pierce) according to the protocol of the manufacturer, rabbits were immunized with this conjugate.

Monoclonal rat anti-dipeptidyl peptidase IV (DPPIV) antibody De 13.4 (16) was kindly provided by Dr. W. Reutter (Freie Universität, Berlin, Germany). Goat anti-rabbit secondary antibodies coupled to Texas Red were purchased from Dianova (Hamburg, Germany), and goat anti-mouse secondary antibodies coupled to Cy_2 (cyanin 2-OSU) were from Biotrend (Köln, Germany).

Immunofluorescence Microscopy—Small pieces of rat liver were removed from anesthetized animals and snap-frozen in isopentane, precooled in liquid nitrogen. For single- and double-labeled immunofluorescence microscopy 4–5-μm thick tissue sections were prepared with a cryotome (Leica, Jung CM3000, Nussloch, Germany), air-dried for 2 h, and fixed for 10 min with cooled acetone (−20 °C). For double-labeled immunofluorescence, the primary mouse and rabbit antibodies and the secondary goat anti-mouse and anti-rabbit antibodies, respectively, were applied simultaneously. Application of the primary or secondary antibodies was for 30–45 min. Unbound antibodies were removed by several washes with phosphate-buffered saline. After a final wash with distilled water, the air-dried sections were mounted with Elvanol (Cti, Idstein/Taunus, Germany). Confocal laser scanning fluorescence microscopy was performed with an LSM 410 apparatus (Carl Zeiss, Jena, Germany). The microscope, equipped with appropriate filter combinations, operated with an argon ion (488 nm) and a helium/neon laser (543 nm). Prints were taken from optical sections of 0.8-μm thickness.

Rat and Human Tissues—Male Sprague-Dawley rats (200–300 g) and male Wistar rats (250–350 g) were obtained from Charles River Wiga (Sulzfeld, Germany). EHBR, defective in the secretion of glutathione *S*-conjugates and structurally related amphiphilic anions (9–11), were provided by Dr. T. Horie from the Eisai Pharmaceutical Company, Ibaraki, Japan. This mutant rat strain was derived from a Sprague-Dawley rat colony. Another mutant rat strain, the GY/TR$^-$ mutant (8, 17, 18) was derived from a Wistar rat colony. Based on cross-breeding experiments, the conclusion has been drawn that the mutations in the EHBR and GY/TR$^-$ mutants are at least allelic (19). Male GY/TR$^-$ mutant rats were provided by Dr. F. Kuipers (University of Groningen, Groningen, The Netherlands). Animals were maintained on a standard diet with free access to food and water.

The human liver sample was obtained perioperatively from excised hepatic tissue from a patient suffering from primary hepatocellular carcinoma. Only healthy liver tissue was used for isolation of total RNA.

Membrane Vesicle Preparation and Measurement of ATP-dependent [^{3}H]LTC$_4$ Transport—Plasma membrane vesicles enriched in hepatocyte canalicular or basolateral membrane domains from Sprague-Dawley and Wistar rat liver were prepared as described elsewhere (7, 20). Transport of [^{3}H]LTC$_4$ (50 nM) into membrane vesicles was determined for 2 min and discontinued by the rapid filtration method as described previously (3, 20).

Isolation of RNA from Tissues—Total RNA was isolated from freeze-clamped tissues by a guanidinium thiocyanate lysis procedure with subsequent centrifugation in cesium chloride solution (21). In brief, frozen pieces of tissues (up to 4 g) were powdered under liquid nitrogen and subsequently homogenized (Ultraturrax T25, Janke & Kunkel IKA-Labortechnik, Staufen i. Br., Germany) for 1 min in 10 ml of lysis buffer containing 4 M guanidinium thiocyanate, 0.5% (w/v) sodium laurylsarcosine, 25 mM trisodium citrate, 0.1 M β-mercaptoethanol. After centrifugation at 10,000 × *g* for 15 min, 8–9 ml of the supernatants were layered onto 3 ml of a cesium chloride solution (5.7 M CsCl, 100 mM EDTA, pH 8.0) and subsequently centrifuged at 180,000 × *g* in a SW-40 Ti Beckman rotor for 20 h at 18 °C. The clear pellet was dissolved in 200–500 μl of diethyl pyrocarbonate-treated water. The RNA was once precipitated with ethanol, washed with 70% ethanol, and finally dissolved in 100–200 μl of diethyl pyrocarbonate-treated water.

Poly(A)$^+$-enriched RNA was isolated from frozen rat liver using the Stratagene mRNA isolation kit according to the manufacturer's instructions (Stratagene, La Jolla, CA).

3′-RACE Studies and RT-PCR Experiments—RT-PCR was performed as described in detail recently (7). In order to analyze the 3′-end sequences of rat liver *mrp* and of human liver *cMRP* (cDNAs), 5 μg of total liver RNA from each liver were reverse transcribed in a 50 μl of transcription buffer (50 mM Tris, pH 8.3, 75 mM KCl, 3 mM $MgCl_2$, 10 mM dithiothreitol, 1 mM dNTPs, 40 units of RNasin) in the presence of 5 μg of oligo(dT)-adapter primer (OWM30) with 50 units of Strata-Script™ reverse transcriptase at 37 °C for 1 h. The reaction was terminated by heating at 95 °C for 5 min followed by immediate cooling on ice. To remove excessive amounts of salt and oligo(dT)-adapter primer, the reaction mixture was subsequently diluted by addition of 2 ml of water and concentrated to a final volume of about 100 μl by the use of Microcon™100 (Amicon, Inc., Beverly, MA). First round PCR was performed in a total volume of 50 μl of PCR buffer (10 × reaction buffer as provided by the manufacturer) containing 1.5 mM $MgCl_2$, 1.25 units of *Taq* DNA polymerase, 0.25 μM sense and antisense primer, and 5 μl of reverse transcription mixture.

Primers used for 3′-RACE experiments were as follows: oligo(dT)-adapter primer (OWM30), 5′-AAGGATCCGTCGACTGCAGAATTC-AAGCTT$(T)_{17}$-3′, adapter primer 1 (OWM31), 5′-AAGGATCC-GTCGACTGC-3′, adapter primer 2 (OWM32), 5′-CGACTGC-AGAATTCAAGCT-3′, the two rat *mrp*-specific sense primers (ForII-4440), 5′-TGCCTGACAAGCTGAACCAT-3′, and (ForI/II-4467), 5′-CAGAAGGTGGAGAGAATCTGA-3′, the two human *cMRP*-specific sense primers (cMRP-N1), 5′-GGAGCTGGCTCACCTCAA-3′, and (cMRP-N2), 5′-CTCAAGTCTTTTGTGGCCA-3′.

In the case of the rat *mrp* 3′-RACE, the ForII-4440 primer was used as sense primer and OWM31 as antisense primer. The PCR was run at a denaturation temperature of 94 °C for 1 min, at an annealing temperature of 50 °C for 1 min, and at an elongation temperature of 72 °C for 1.5 min, for a total of 35 cycles. The reaction was completed by a 10-min incubation at 72 °C. Subsequently, nested PCR was performed with 1 μl of the first round PCR using ForI/II-4467 as sense and OWM32 as antisense primer under the same conditions as described for first round PCR, except that the annealing temperature was raised to 52 °C. In the case of the human *cMRP* 3′-RACE, first round PCR was driven with cMRP-N1 as sense and OWM31 as antisense primer. The nested PCR was driven with cMRP-N2 as sense and OWM32 as antisense primer. Reactions were performed under conditions as outlined for rat *mrp* 3′-RACE.

Northern Blot Analysis—If not stated otherwise, formamide-denatured poly(A)$^+$-RNA was fractionated by electrophoresis on a 1.2% formaldehyde-containing agarose gel, transferred to Duralon-UV™ membranes (Stratagene) with 10 × SSC buffer (1.5 M NaCl, 0.15 sodium citrate, pH 7.0), prehybridized for 1 h at 68 °C, and hybridized for 18 h at 68 °C with the nick-translated 347 bp cDNA probe from rat liver (7), (*cmrp* corresponding to *seq1*) prepared by RT-PCR as described recently (7). A rat β-actin probe served as a control. The size of RNA was estimated by the Molecular Weight Marker II (Boehringer Mannheim, Mannheim, Germany). Nick-translation was performed with the Rediprime DNA labeling system (Amersham-Buchler, Braunschweig, Germany) according to the instructions of the manufacturer. The membrane was washed under high stringency conditions once in 1 × SSC buffer (see above), 0.1% SDS, once in 0.5 × SSC, 0.1% SDS, and once in 0.1 × SSC, 0.1% SDS, each at 65 °C for 20 min. The blots were dried, and autoradiography was performed at −80 °C with an intensifying screen for one (β-actin) and 4 days (*seq1*), respectively.

Construction and Screening of a Rat Liver cDNA Library—A unidirectional cDNA library in the Uni-ZAP™ XR vector was made using 6 μg of rat liver poly(A)$^+$-enriched RNA (mRNA) and the ZAP-cDNA® system (Stratagene, Heidelberg, Germany) according to the manufacturer's instructions. In brief, the mRNA was reverse transcribed by means of an *Xho*I-linked poly(dT) primer in the presence of a nucleotide mixture containing 5-methyl dCTP. After completion of the second strand synthesis by the use of DNA polymerase I and RNase H, uneven termini of double-stranded cDNAs were filled in with cloned *Pfu* DNA polymerase, and then *Eco*RI adapters were ligated to the blunt ends. *Xho*I digestion released the *Eco*RI adapter and residual linker-primer from the 3′-end of the cDNA. cDNA was size-fractionated using Sephacryl® S-500 spin-columns, precipitated, and ligated into the *Xho*I- and *Eco*RI-restricted Uni-ZAP XR vector. Following ligation, the library was packaged into λ phages by the use of Gigapack III Gold packaging extract (Stratagene, Heidelberg, Germany). The primary library, containing approximately 1.7 × 10^6 independent clones with an average insert size of about 2 kb, was amplified without delay. This amplified library was screened in a first round by plaque hybridization using the recently described 347-bp RT-PCR fragment from rat liver cDNA (*seq1* (7); see also "Results"). The fragment was labeled as described under "Northern Blotting." The plaque hybridizations were performed at

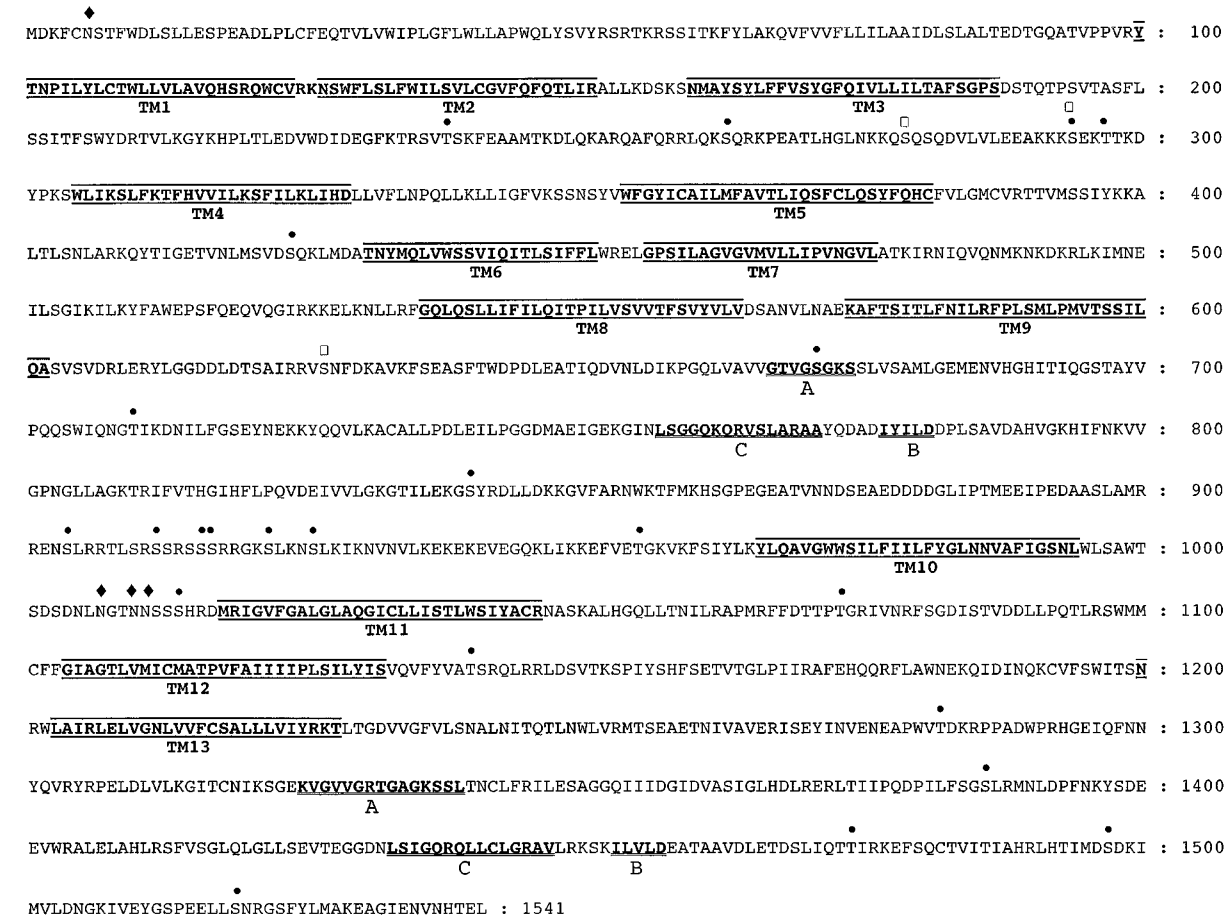

FIG. 1. **Deduced amino acid sequence of rat cMrp.** The amino acid sequence was deduced from the nucleotide sequence of the full-length cDNA clone (accession no. X96393 in the EMBL/GenBank™/DDBJ data bases). The transmembrane segments predicted by the TMAP program (26) are marked in bold with lines above and below (*TM1–13*). The predicted nucleotide-binding domains with the Walker A and B motifs and the ABC transporter family signature (28, 29) are marked in *bold* and *double underlined*, and indicated by *A*, *B*, and *C*, respectively. The extracellular *N*-glycosylation sites are marked by *closed diamonds*. Possible sites of phosphorylation by protein kinase A (*open squares*) and protein kinase C (*filled circles*) are marked above the sequence.

TABLE I
Sequence comparison of amino acids in cMrp with related ABC transporters

Protein	Amino acids	Identity[a]	Similarity[a]
		%	%
cMrp rat[b]	1541	100	100
MRP human[c]	1531	47.8	67.9
YCF1 yeast[d]	1515	41.9	63.2
YHD5 yeast[e]	1592	32.9	57.8
Sur rat[f]	1582	32.4	54.8
CFTR human[g]	1481	30.1	55.7
Mdr2 rat[h]	1278	23.7	50.0
MDR1 human[i]	1280	22.8	50.0

[a] Sequence alignments were generated using the BEST program from the HUSAR program package (23).
[b] See Fig. 1.
[c] Cole *et al.* (1).
[d] Szczypka *et al.* (12).
[e] Johnston *et al.* (30).
[f] Aguilar-Bryan *et al.* (31).
[g] Riordan *et al.* (32).
[h] Brown *et al.* (33).
[i] Chen *et al.* (34).

68 °C in hybridization buffer (6 × SSC, 5 × Denhardt's reagent, 0.1% SDS, 100 μg/ml sheared denatured salmon sperm DNA) followed by three high stringency washing steps (1 × SSC, 0.1% SDS; 0.5 × SSC, 0.1% SDS; 0.1 × SSC, 0.1% SDS; each at 68 °C for 20 min). Positive clones were then plaque-purified by secondary and tertiary screening and the pBluescript phagemid, containing the *cmrp* insert was obtained by the *in vivo* excision procedure. The first round of hybridization yielded several *cmrp* clones with sizes up to 3.4 kb. A second rat liver cDNA library screening was performed using the *Eco*RI-*Bam*HI 5′-restriction fragment (693 bp) of the longest first-round *cmrp* clone as probe. This screening yielded a full-length *cmrp* clone of 4.9 kb.

DNA Sequencing—The cDNA clones were sequenced by the dideoxynucleotide chain termination method of Sanger (22) using [α-^{35}S]dATP and the sequencing kit from Pharmacia Biotech Inc. (Freiburg, Germany). Dried gels were exposed to Kodak BioMax MR-1 film (Sigma).

The HUSAR program (23) based on the Wisconsin Genetics Computer Group (GCG) program package (24) was used for computer analysis during this study. Further details are given under "Results."

Immunoblot Analysis of Proteins—Membrane fractions (25 μg of protein) were loaded onto a 7.5% (w/v) SDS-polyacrylamide gel electrophoresis (25), without boiling, and subjected to electrophoresis. After electrotransfer onto nitrocellulose membranes (Schleicher & Schuell, Dassel, Germany) the blots were blocked with Tris-buffered saline containing 0.05% Tween 20 and 5% bovine serum albumin for 1 h at room temperature and probed overnight with the polyclonal anti-cMrp antibody EAG15 (dilution 1:40,000), raised against the carboxyl-terminal peptide of cMrp. Antibody binding was visualized with horseradish peroxidase-conjugated goat anti-rabbit antibody (Bio-Rad, München, Germany) diluted 1:1000, followed by enhanced chemiluminescence detection (Amersham-Buchler, Braunschweig, Germany) with exposure on Hyperfilm-MP.

RESULTS

Cloning of the cDNA Encoding the Hepatocyte Canalicular Conjugate Export Pump—The rat liver λ-ZAP cDNA library was screened for isolation of the cDNA encoding the hepatocyte canalicular export pump and several clones were isolated by

TABLE II
Comparison of peptide domains in ABC transporters with cMrp
Sequence alignments were generated using the BEST program from the HUSAR program package (23).

	Domain[a] (peptide)	Amino terminus (1–96)	TM I (97–648)	NBD1 (649–798)	Linker region (799–960)	TM II (961–1301)	NBD2 (1302–1474)	Carboxyl terminus (1475–1541)
				%				
cMrp rat	Identity or similarity	100	100	100	100	100	100	100
MRP human[b]	Identity	29.8	40.2	66.7	36.2	47.8	73.3	61.0
	Similarity	57.4	61.3	82.7	57.1	70.3	84.9	78.0
YCF1 yeast[c]	Identity	21.8	34.0	54.0	27.1	46.3	63.4	58.7
	Similarity	57.5	56.9	70.0	51.4	66.5	77.9	82.5
Sur rat[d]	Identity	27.3	25.3	43.6	25.2	32.5	51.2	43.1
	Similarity	56.8	49.4	66.4	45.7	53.3	71.5	65.5

[a] Domains for this multisequence alignment are defined with respect to the amino acid position in cMrp (Fig. 1). TM I designates the peptide comprising transmembrane segments 1–9 and TM II comprises transmembrane segments 10–13. NBD 1 and NBD 2 designate the first and second nucleotide-binding domains, respectively.
[b] Cole *et al.* (1).
[c] Szczypka *et al.* (12).
[d] Aguilar-Bryan *et al.* (31).

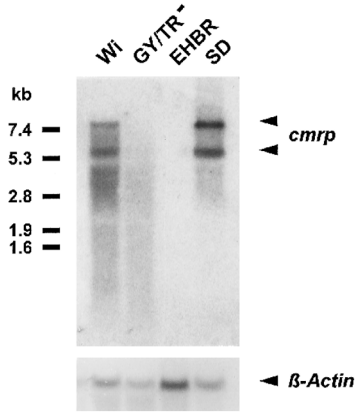

FIG. 2. **Northern blot analysis of *cmrp* expression in normal and mutant rat livers.** Each lane contains 5 μg of poly(A)$^+$ RNA from liver of EHBR and GY/TR$^-$ mutant rats and the corresponding wild-type strains Sprague-Dawley (*SD*) and Wistar (*Wi*). The RNA was first hybridized with the 347-bp cDNA fragment of *cmrp* (*seq1*) (7) under high stringency conditions and reprobed with a rat β-actin cDNA fragment as outlined under "Experimental Procedures." Autoradiographs are a 4-day and 1-day exposure for *cmrp* and β-actin, respectively. Only RNA from the wild-type rat strains (Wi and SD) gave two distinct bands.

using the 347-bp cDNA fragment *seq1* (7). Restriction analyses indicated that clone CM23 showed the largest insert with about 3.4 kb in length. A second plaque hybridization was performed using the 5′-located *Eco*RI-*Bam*HI restriction fragment of clone CM23. This screening led to clone CM2.1, with an insertion length of 4.9 kb, and to clone CM2.17 with an insertion length of 4.6 kb. The entire insert of clone CM2.1 was sequenced from both strands and revealed a first in-frame ATG codon located at nucleotides 50–52, followed by a stop codon located at positions 4673–4675. The sequence context around the ATG translational start codon was $^{-3}$ATT**ATG**G^{+4} and fulfilled the Kozak consensus (27) with the invariant A at position −3 and the usual G at position +4. Two putative polyadenylation sites with the consensus sequence AATAAA were located at positions 4866–71 and 4878–83.

Analysis of the Deduced Amino Acid Sequence of cMrp—The open reading frame of 4623 bp encodes a predicted protein of 1541 amino acids (Fig. 1) with a calculated molecular mass of 173,318 Da, which has been given the name cMrp (for *c*analicular *m*ultidrug *r*esistance *p*rotein). A BLASTP search of the Swissprot data base showed that cMrp exhibits striking sequence similarities with various ABC proteins (Table I). The sequence of cMrp has significant similarities with the amino acid sequences of human MRP (1), the cadmium resistance protein YCF1 from yeast (12), the putative yeast permease YHD5 (30), the sulfonyl urea receptor (31), the cystic fibrosis transmembrane conductance regulator CFTR (32), and with lower similarity and identity scores, with the Mdr2 P-glycoprotein (33), and with the MDR1 P-glycoprotein (34) (Table I). The amino acid sequence deduced from the *cmrp* cDNA contained the structural features consistent with a protein composed of two homologous halves, typical for the ABC transporter proteins. Each half contained the transmembrane domains (TMI and TMII in Table II) and the structural motifs (28, 29) for putative ATP-binding sites including the Walker A and B motifs and the putative consensus pattern for the ABC transporter family signature (*C*) (Fig. 1). The high sequence similarity, especially in the two nucleotide-binding domains and in the carboxyl-terminal part, between cMrp, MRP (1), and YCF1 (12) is outlined in Table II. The pattern in the second nucleotide-binding domain (amino acids 1433–1447) also fulfilled the consensus pattern for the ABC transporter family signature (C) except for the isoleucine in position 1435. Analysis by the use of the TMAP program for prediction of transmembrane segments in proteins (26) revealed at least 13 transmembrane segments for the cMrp sequence (Fig. 1). This analysis was based on a CLUSTAL sequence alignment file (35) and included cMrp (Fig. 1), human MRP (1), and the rat sulfonyl urea receptor (Sur) protein (31). Interestingly, the TMAP program (26) led to a prediction of a 9 plus 4 distribution of the transmembrane segments (Fig. 1), rather than a 8 plus 4 distribution described earlier for MRP by the use of a different algorithm (1, 37). The 9 plus 4 distribution corresponds to the transmembrane segment prediction for the sulfonyl urea receptor (Sur) protein (31) suggesting an extracellular location of the N-terminal domain of the protein (37). TMAP analysis using alignments which included the yeast cadmium resistance factor YCF1 (12) and the supposed ATP-dependent permease YHD5 from yeast (30) led to a prediction of 14 transmembrane segments. However, only the positions and the number of the first two transmembrane segments are affected by these different TMAP predictions. The cMrp sequence contained 11 predicted *N*-glycosylation sites of which three were located on the predicted extracellular loop between transmembrane segments 10 and 11, and, as in the human MRP and the rat sulfonyl urea receptor (Sur) protein, a single *N*-glycosylation site was predicted on the extracellular domain near the amino terminus of cMrp (Fig. 1). In addition, the sequence between the first nucleotide-binding domain and the TM II domain, defined in Table II and commonly referred to as the linker region, is characterized by a high content of about 38% charged amino acids and several consensus sequences for phosphorylation by

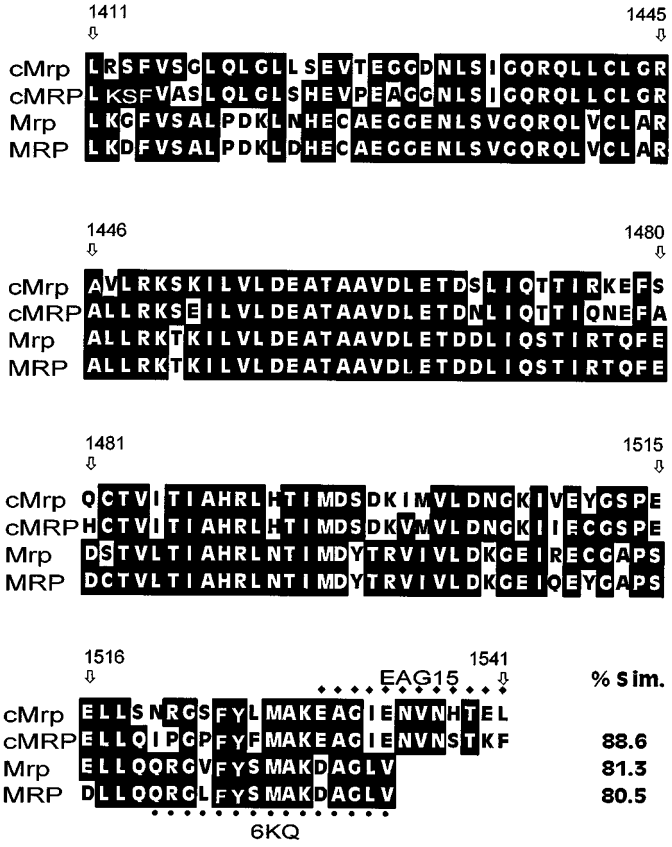

FIG. 3. **Deduced carboxyl-terminal sequences of rat cMrp and Mrp, and human cMRP and MRP.** The corresponding nucleotide sequences of the rat *mrp* and the human *cMRP* were obtained by the 3′-RACE technique. The rat *cmrp* sequence (see Fig. 1) was cloned as outlined under "Experimental Procedures"; the human *MRP* sequence (1) is from the EMBL Data Bank (L05628). The sequences were aligned by the CLUSTAL program from the HUSAR program package (23, 24, 35). Boxes (*black background*) indicate that at least two amino acids are identical at this position. Similarity scores for these carboxyl-terminal sequences relative to cMrp are indicated (*Sim.*) in the figure; identity scores relative to cMrp are as follows: human cMRP, 80.2%; rat Mrp, 65.8%; and human MRP, 66.7%. The peptide sequences recognized by the polyclonal antibodies 6KQ (36) and EAG15 are indicated by dots and diamonds, respectively. Numbers indicate the amino acid position corresponding to cMrp.

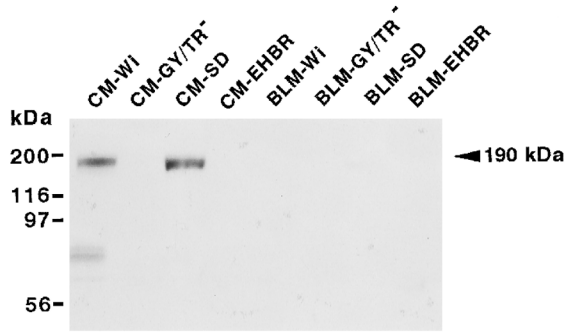

FIG. 4. **Detection of cMrp in normal and transport-deficient rat hepatocyte membranes.** Immunoblot analysis of cMrp in bile canalicular (*CM*) and basolateral (*BLM*) hepatocyte membrane preparations from transport-deficient EHBR and GY/TR$^-$ mutants and from the wild-type Sprague-Dawley (*SD*) and Wistar (*Wi*) rats, respectively. Membrane fractions (50 μg of protein) were subjected to 7.5% SDS-polyacrylamide gel electrophoresis and subsequently transferred to nitrocellulose membranes as described under "Experimental Procedures." The protein blots, probed with the EAG15 antibody raised against the carboxyl-terminal peptide sequence of rat cMrp (Fig. 3), indicated a band at 190 kDa in the normal rat livers.

cAMP-dependent protein kinase A and protein kinase C (Fig. 1).

Northern Blot Analysis of cmrp Expression in Normal and Mutant Rat Liver—The question whether the lack of amplification of *cmrp* cDNA in the transport-deficient GY/TR$^-$ mutant rat (7) was due to point mutations within the primer target sites or possibly due to a lack of the corresponding mRNA was studied by analysis of the expression of the *cmrp* gene by Northern blot hybridization (Fig. 2). Poly(A)$^+$-enriched RNA from liver tissues from GY/TR$^-$ and EHBR mutant rats, as well as from normal Wistar and normal Sprague-Dawley rats, was probed using the 347-bp *cmrp* cDNA fragment *seq1* (7). The rat *cmrp* cDNA fragment hybridized to two mRNAs of about 5.5 and 7.5 kb (Fig. 2). Interestingly, the *seq1* cDNA fragment hybridized only with mRNA from normal Sprague-Dawley and normal Wistar rat liver, whereas liver of both mutants, EHBR and GY/TR$^-$, lacked the corresponding mRNA (Fig. 2). These findings indicate that the defects in EHBR and GY/TR$^-$ mutant rats are caused by a lack of expression or by rapid degradation of the *cmrp* mRNA detected by the *seq1* cDNA probe.

Comparison of the Deduced Carboxyl-terminal Amino Acid Sequences of Rat cMrp, Human cMRP, Rat Mrp, and Human MRP—The purified polyclonal 6KQ antibody, raised against the peptide at the carboxyl terminus of human MRP (36), indicated the absence of the canalicular isoform of Mrp in the GY/TR$^-$ mutant rat (7) as well as the absence of the human cMRP in the liver of a patient with Dubin-Johnson syndrome (13). 3′-RACE studies with rat and human liver mRNA, using primer systems targeted against the highly conserved second nucleotide-binding domain of these *MRP* sequences (see "Experimental Procedures"), served to identify the carboxyl-terminal sequence of rat liver Mrp and human liver cMRP (Fig. 3). Alignment of the carboxyl termini of these 4 ABC transporters of the MRP family indicated a high degree of sequence similarity of Mrp and cMrp from rat liver with the sequences of human MRP (Table II) and human liver cMRP, respectively (Fig. 3). Furthermore, the sequence analysis supported the immunological observations (7) mentioned above on the reactivity of the 6KQ antibody (36), because of the high sequence similarity in the antigenic peptide part against which the 6KQ antibody had been raised (see Fig. 3, marked by *dots*).

Immunoblot Analysis of cMrp in Rat Liver Membranes—We have raised the polyclonal EAG15 antibody against the peptide of 12 amino acids at the carboxyl terminus of cMrp (Fig. 3, *closed diamonds*) in order to differentiate between rat Mrp and its hepatocyte canalicular isoform cMrp. Immunoblot analyses were performed with canalicular and basolateral membrane preparations from the GY/TR$^-$ and EHBR mutants and from their corresponding normal Wistar and Sprague-Dawley counterparts. The EAG15 antibody detected a protein of about 190 kDa exclusively in the canalicular membrane of the normal liver (Fig. 4). The protein was not detectable in membranes from GY/TR$^-$ and EHBR mutants, even after enhancement of the sensitivity by an extended exposure time of the blot (Fig. 4). Exposure of the blot for longer time periods in the enhanced chemiluminescence detection system indicated small amounts of the 190-kDa protein in the basolateral membrane preparation which results from its known contamination with canalicular membranes (7). Furthermore, faint bands were visible at 60–70 kDa after long term exposure in canalicular membranes from normal liver but not in the membranes from EHBR and GY/TR$^-$ mutants, suggesting carboxyl-terminal peptide degradation products of cMrp. Deglycosylation of rat liver canalicular membrane preparations by glycopeptide *N*-glycosidase under conditions described recently (7) reduced the apparent molecular weight of cMrp, detected on the immunoblot by the

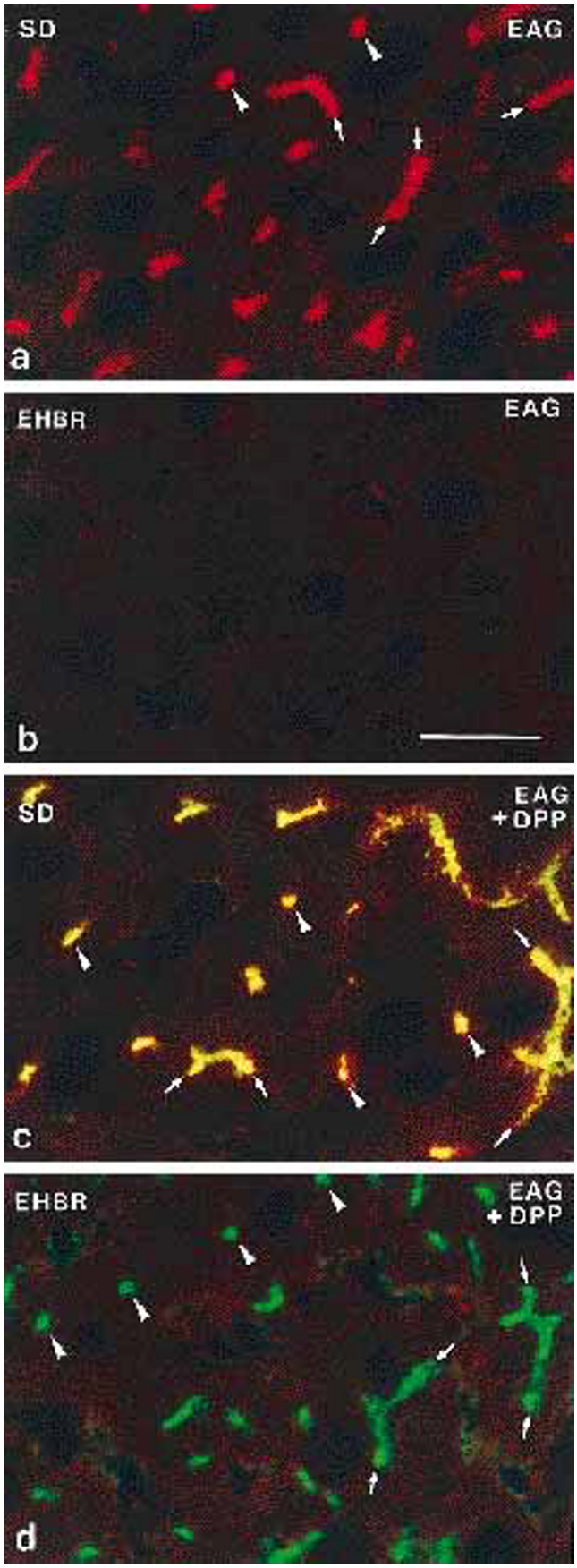

FIG. 5. **Confocal laser scanning micrographs of normal and mutant rat liver.** Frozen sections of normal Sprague-Dawley (*SD*; *a* and *c*) and EHBR mutant liver (*EHBR*; *b* and *d*) after reaction with the EAG15 (*EAG*) antibody (*a* and *b*) and after simultaneous application of the EAG15 and the anti-DPPIV (*DPP*) antibodies (*c* and *d*). Note that the presence of both antigens, cMrp and DPPIV, in the bile canalicular membrane of normal liver results in a yellow color mixture of the red staining and green reaction product (*c*), while the absence of cMrp in the EHBR mutant liver is documented in the double-labeled immunofluorescence experiment by the green reaction product of the anti-DPPIV antibody (*d*). *Arrows* point to longitudinally, *arrowheads* to cross-sectioned bile canaliculi. *Bar*, 20 μm.

EAG15 antibody, from 190 kDa to about 170 kDa (figure not shown).

Confocal Laser Scanning Microscopy—Application of the EAG15 antibody revealed on cryosections of normal rat liver positive reactions in the form of small spots and irregularly shaped elongated structures (Fig. 5*a*). An identical staining pattern was observed when the monoclonal antibody De 13.4 directed against dipeptidyl peptidase (DPPIV) and recognizing canalicular (apical) membrane domains (16) was applied (not shown). Double-label experiments using the EAG15 and anti-DPPIV antibodies confirmed that both antibodies recognized antigens localized in bile canalicular structures of normal rat liver sections, since the superimposition of the two different fluorescent dyes used to visualize the two different antibodies resulted in a yellow color, thus indicating complete colocalization (Fig. 5*c*). The EAG15 antibody applied to liver sections of EHBR mutants did not show any reaction (Fig. 5*b*). Consequently, double-labeled experiments with the EAG15 and anti-DPPIV antibodies on liver sections of EHBR mutants resulted in a clear green staining of the bile canalicular membrane areas due to the recognition of only DPPIV (Fig. 5*d*).

ATP-dependent [^{3}H]LTC$_4$ Transport into Membrane Vesicles of Normal and EHBR Mutant Rats—The deficient transport in the EHBR mutants was confirmed by measurement of ATP-dependent transport of [^{3}H]LTC$_4$ into inside-out oriented liver plasma membrane vesicles (Table III). In order to differentiate between binding of the labeled substrate and ATP-dependent uptake into the vesicles, transport was performed by incubation of the membrane vesicles with 50 nM [^{3}H]LTC$_4$ in the presence of 4 mM ATP or 4 mM 5′-AMP (2, 3, 7, 20). The net ATP-dependent uptake of [^{3}H]LTC$_4$ by canalicular membrane vesicles from EHBR liver was below 3% of normal, and the residual transport was not significantly affected by a potent and selective inhibitor of the MRP-mediated transport (3), the LTD$_4$-receptor antagonist MK571 (38). The anionic quinoline derivative MK571 effectively inhibited [^{3}H]LTC$_4$ transport into membrane vesicles prepared from normal liver (Table III). The residual transport activity in the basolateral membrane preparation from normal Sprague-Dawley rat liver most probably resulted from contamination of the preparation with canalicular membrane vesicles (7). This residual transport was also effectively inhibited by MK571.

DISCUSSION

Recently we studied the expression of the human *MRP* gene and of the rat *mrp* gene in liver by PCR amplification of cDNA reverse transcribed from poly(A)$^+$ RNA using degenerate primer pairs derived from highly conserved regions in the second nucleotide-binding domain of the human *MRP* gene and the *Leishmania ltpgpA* gene (7). In this recent study we sequenced two different 347-bp cDNA fragments from rat liver, termed *seq1* and *seq2* (7), which exhibited a high degree of sequence similarity with the human *MRP* cDNA (1). Our present work demonstrates that the *seq1* sequence (7) has been part of a novel cDNA encoding a membrane glycoprotein (Fig. 1) of the ABC superfamily of transporters. Based on the amino acid sequence similarity with other ABC proteins, the canalicular isoform cMrp (Fig. 1) is related next to MRP (1) (67.9% overall

TABLE III

ATP-dependent leukotriene C_4 transport activity in canalicular and basolateral membrane vesicle preparations from normal Sprague-Dawley (SD) and EHBR mutant rat liver

ATP-dependent transport of LTC_4 (50 nM) was measured in the absence or presence of 5 μM MK571, an established inhibitor of MRP-mediated transport of LTC_4 (2, 3). Mean values ± S.E. from four determinations.

Membrane	ATP-dependent LTC_4 transport	
	−MK571	+MK571
	pmol × mg protein^{-1} × min^{-1} (%)	
SD (canalicular)	16.1 ± 0.7 (100)	3.1 ± 0.5 (19)
SD (basolateral)	4.8 ± 0.4 (30)	0.8 ± 0.4 (5.0)
EHBR (canalicular)	0.4 ± 0.2 (2.5)	0.3 ± 0.2 (1.9)
EHBR (basolateral)	0.9 ± 0.5 (5.6)	0.7 ± 0.4 (4.3)

similarity), to the yeast cadmium resistance factor YCF1 (12) (63.2% similarity), to the yeast permease YHD5 (30) (57.8% similarity), to the sulfonyl urea receptor (Sur) (31) (54.8% similarity), and to the cystic fibrosis transmembrane conductance regulator (CFTR) chloride channel (32) (55.7% similarity) (Table I). The prediction of 13 transmembrane segments (Fig. 1) by the TMAP program (26) is in line with the recent sequence analysis of the sulfonyl urea receptor (Sur) protein (31). In both proteins, Sur (31) and cMrp (Fig. 1), four transmembrane segments were consistently predicted between the two ATP-binding domains. However, the predicted placement of the amino-terminal peptide to the extracellular domain in both cMrp (Fig. 1) and Sur (31) differs from the canonical model for the ABC transporter superfamily and requires additional studies and further confirmation.

Northern blot analysis, using the 347-bp *seq1* cDNA fragment (7), showed the lack of *cmrp* mRNA in the EHBR and the GY/TR$^-$ mutant rats (Fig. 2). These results were consistent with the immunoblot analyses (Fig. 4) and with the immunofluorescence microscopy studies demonstrating that the 190-kDa protein was exclusively localized to the canalicular membrane of hepatocytes and was absent in both mutant rat strains (Fig. 5). Therefore, the function of cMrp can be defined on the basis of its hereditary deficiency in the EHBR (Figs. 2, 4, and 5) and the GY/TR$^-$ (Figs. 2 and 4) mutant rats which lack the capacity for ATP-dependent transport of amphiphilic anions across the hepatocyte canalicular membrane (7, 8, 11, 39). Additional analyses of the deficient hepatobiliary elimination of substances from the liver into bile in both mutant strains have indicated a wide range of conjugates and organic anions to be substrates for the *cmrp*-encoded canalicular export pump (7–11, 17–18, 40). The export pump deficient in the GY/TR$^-$ mutant rat has been termed canalicular multispecific organic anion transporter (cMOAT) (8), or non-bile acid organic anion transporter (41), or glutathione S-conjugate export pump or leukotriene export pump (39). The latter term refers to the endogenous glutathione *S*-conjugate LTC_4 which is the substrate with an affinity for this transporter in the nanomolar concentration range (39, 42). We have confirmed in this study (Table III) that the ATP-dependent transport of LTC_4 is deficient in canalicular membrane vesicles from EHBR mutant liver (11), as it is the case in canalicular membranes from GY/TR$^-$ mutant liver (7, 39). It is of interest that MK571, a selective and potent inhibitor of MRP-mediated LTC_4 transport (2, 3), also effectively inhibited the canalicular transport mediated by the *cmrp*-encoded conjugate export pump (Table III). Taken together, the present state of information indicates that the inhibitor and the substrate specificity of recombinant human MRP (3, 6) and of rat cMrp are very similar, in spite of major differences in the amino acid sequence of both transporters (Tables I and II). It will be of interest to define the common structural motifs determining the substrate and inhibitor specificity of the conjugate export pumps encoded by the *cmrp* and the *MRP* genes. In analogy to the multidrug resistance caused by overexpression of MRP (1, 36, 43), it is conceivable that overexpression of human cMRP and rat cMrp in tumor cells, particularly in hepatocellular carcinomas, also causes multidrug resistance.

Acknowledgments—We thank Ulrike Buchholz, Jutta Arlt, and Rosmarie Mayer, Heidelberg, for their expert experimental support.

REFERENCES

1. Cole, S. P. C., Bhardwaj, G., Gerlach, J. H., Mackie, J. E., Grant, C. E., Almquist, K. C., Stewart, A. J., Kurz, E. U., Duncan, A. M., and Deeley, R. G. (1992) *Science* **258,** 1650–1654
2. Jedlitschky, G., Leier, I., Buchholz, U., Center, M., and Keppler, D. (1994) *Cancer Res.* **54,** 4833–4836
3. Leier, I., Jedlitschky, G., Buchholz, U., Cole, S. P. C., Deeley, R. G., and Keppler, D. (1994) *J. Biol. Chem.* **269,** 27807–27810
4. Müller, M., Meijer, C., Zaman, G. J. R., Borst, P., Scheper, R. J., Mulder, N. H., De Vries, E. G. E., and Jansen, P. L. M. (1994) *Proc. Natl. Acad. Sci. U. S. A.* **91,** 13033–13037
5. Leier, I., Jedlitschky, G., Buchholz, U., Center, M., Cole, S. P. C., Deeley, R. G., and Keppler, D. (1996) *Biochem. J.* **314,** 433–437
6. Jedlitschky, G., Leier, I., Buchholz, U., Barnouin, K., Kurz, G., and Keppler, D. (1996) *Cancer Res.* **56,** 988–994
7. Mayer, R., Kartenbeck, J., Büchler, M., Jedlitschky, G., Leier, I., and Keppler, D. (1995) *J. Cell Biol.* **131,** 137–150
8. Oude Elferink, R. P. J., Meijer, D. K. F., Kuipers, F., Jansen, P. L. M., Groen, A. K., and Groothuis, G. M. M. (1995) *Biochim. Biophys. Acta* **1241,** 215–268
9. Takikawa, H., Sano, N., Narita, T., Uchida, Y., Yamanaka, M., Horie, T., Mikami, T., and Tagaya, O. (1991) *Hepatology* **14,** 352–360
10. Hosokawa, S., Tagaya, O., Mikami, T., Nozaki, Y., Kawaguchi, A., Yamatsu, K., and Shamoto, M. (1992) *Lab. Anim. Sci.* **42,** 27–34
11. Fernández-Checa, J. C., Takikawa, H., Horie, T., Ookhtens, M., and Kaplowitz, N. (1992) *J. Biol. Chem.* **267,** 1667–1673
12. Szczypka, M. S., Wemmie, J. A., Moye-Rowley, W. S., and Thiele, D. J. (1994) *J. Biol. Chem.* **269,** 22853–22857
13. Kartenbeck, J., Leuschner, U., Mayer, R., and Keppler, D. (1996) *Hepatology* **23,** 1061–1066
14. Roy Chowdhury, J., Roy Chowdhury, N. R., Wolkoff, A. W., and Arias I. M. (1994) in *The Liver: Biology and Pathobiology* (Arias, I. M., Boyer, J. L., Fausto, N., Jakoby, W. B., Schachter, D., and Shafritz, D., eds) pp. 471–504, Raven Press, New York
15. Schnölzer, M., Alewood, P., Jones, A., Alewood, D., and Kent, S. B. H. (1992) *Int. J. Pept. Protein Res.* **40,** 180–193
16. Becker, A., Neumeier, R., Heidrich, C., Loch, N., Hartel, S., and Reutter, W. (1986) *Biol. Chem. Hoppe-Seyler* **367,** 681–688
17. Jansen, P. L. M., Peters, W. H. M., and Lamers, W. H. (1985) *Hepatology* **5,** 573–579
18. Kuipers, F., Enserink, M., Havinga, R., Van der Steen, A. B. M., Hardonk, M. J., Fevery, J., and Vonk, R. J. (1988) *J. Clin. Invest.* **81,** 1593–1599
19. Nishida, T., Hardenbrook, C., Gatmaitan, Z., and Arias, I. M. (1992) *Am. J. Physiol.* **262,** G629–G635
20. Böhme, M., Müller, M., Leier, I., Jedlitschky, G., and Keppler, D. (1994) *Gastroenterology* **107,** 255–265
21. Chirgwin, J. M., Przybyla, A. E., MacDonald, R. J., and Rutter, W. J. (1979) *Biochemistry* **18,** 5294–5299
22. Sanger, F., Coulson, A. R., Barrell, B. G., Smith, A. J. H., and Roe, B. A. (1980) *J. Mol. Biol.* **143**, 161–178
23. Senger, M., Glatting, K. H., Ritter, O., and Suhai, S. (1995) *Comput. Methods Programs Biomed.* **46,** 131–141
24. Devereux, J., Haeberli, P., and Smithies, O. (1984) *Nucleic Acids Res.* **12,** 387–395
25. Laemmli, U. K. (1970) *Nature* **227,** 680–685
26. Persson, B., and Argos, P. (1994) *J. Mol. Biol.* **237,** 182–192
27. Kozak, M. (1984) *Nucleic Acids Res.* **12,** 857–872
28. Higgins, C. F., Gallagher, M. P., Mimmack, M. L., and Pearce, S. R. (1988) *Bioessays* **8,** 111–116
29. Hyde, S. C., Emsley, P., Hartshorn, M. J., Mimmack, M. M., Gileadi, U., Pearce, S. R., Gallagher, M. P., Gill, D. R., Hubbard, R. E., and Higgins, C. F. (1990) *Nature* **346,** 362–365
30. Johnston, M., Andrews, S., Brinkman, R., Cooper, J., Ding, H., Dover, J., Du, Z., Favello, A., Fulton, L., Gattung, S., Geisel, C., Kirsten, J., Kucaba, T., Hillier, L., Jier, M., Johnston, L., Langston, Y., Latreille, P., Louis, E. J., Macri, C., Mardis, E., Menezes, S., Mouser, L., Nhan, M., Rifkin, L., Riles, L., St. Pepter, H., Trevaskis, E., Vaughan, K., Vignati, D., Wilcox, L., Wohldman, P., Waterston, R., Wilson, R., and Vaudin, M. (1994) *Science* **265,** 2077–2082
31. Aguilar-Bryan, L., Nichols, C. G., Wechsler, S. W., Clement, J. P., Boyd, A. E., III, Gonzalez, G., Herrera-Sosa, H., Nguy, K., Bryan, J., and Nelson, D. A. (1995) *Science* **268,** 423–426
32. Riordan, J. R., Rommens, J. M., Kerem, B., Alon, N., Rozmahel, R., Grzelczak, Z., Zielenski, J., Lok, S., Plavsic, N., Chou, J. L., Drumm, M. L., Iannuzzi, M. C., Collins, F. S., and Tsui, L. C. (1989) *Science* **245,** 1066–1073
33. Brown, P. C., Thorgeirsson, S. S., and Silverman, J. A. (1993) *Nucleic Acids Res.* **21,** 3885–3891
34. Chen, C., Chin, J. E., Ueda, K., Clark, D. P., Pastan, I., Gottesman, M. M., and Roninson, I. B. (1986) *Cell* **47,** 381–389

35. Higgins, D. G., and Sharp, T. M. (1989) *Comput. Appl. Biosci.* **5,** 151–153
36. Krishnamachary, N., Ma, L., Zheng, L., Safa, A. R., and Center, M. S. (1994) *Oncol. Res.* **6,** 119–127
37. Philipson, L. H., and Steiner, D. F. (1995) *Science* **268,** 372–373
38. Jones, T. R., Zamboni, R., Belley, M., Champion, E., Charette, L., Ford-Hutchinson, A. W., Frenette, R., Gauthier, J. Y., Leger, S., Masson, P., McFarlane, S., Piechuta, H., Rokach, J., Williams, H., Young, R. M., DeHaven, R. N., and Pong, S. S. (1989) *Can. J. Physiol. Pharmacol.* **67,** 17–28
39. Ishikawa, T., Müller, M., Klünemann, C., Schaub, T., and Keppler, D. (1990) *J. Biol. Chem.* **265,** 19279–19286
40. Huber, M., Guhlmann, A., Jansen, P. L. M., and Keppler, D. (1987) *Hepatology* **7,** 224–228
41. Arias, I. M., Che, M., Gatmaitan, Z., Leveille, C., Nishida, T., and St. Pierre, M. (1993) *Hepatology* **17,** 318–329
42. Böhme, M., Büchler, M., Müller, M., and Keppler, D. (1993) *FEBS Lett.* **333,** 193–196
43. Cole, S. P. C., Sparks, K. E., Fraser, K., Loe, D. W., Grant, C. E., Wilson, G. M., and Deeley, R. G. (1994) *Cancer Res.* **54,** 5902–5910